Stochastic Modelling and Computational Sciences
Vol. 3 No. 1 (June, 2023)

Received: 20th March 2023 *Revised: 18th May 2023* *Accepted: 30th June 2023*

THE USE OF NUMERICAL MONTE CARLO INTEGRATION TO VERIFY THE PHYSICAL FEASIBILITY OF A TRAJECTORY BASED ON SURVEILLANCE RADAR DATA

A.S. SOLONAR, P.A. KHMARSKI, A.O. NAUMOV, D.A. JURAEV*, AND B.M. MUXAMMEDOV

Abstract. The developed methodology for checking the physical feasibility of a trajectory during its removal phase from automatic tracking in a trajectory processing device based on surveillance radar data is considered. The approach is based on the numerical Monte Carlo integration method, taking into account the altitude-velocity characteristics of real aircraft. It is suggested to describe the a priori trajectory features by means of the generalized Gaussian distribution. The proposed solution makes it possible to improve the quality of selection of real objects observed against the background of target-like interference

1. Introduction

Modern radar facilities are complex real-time information and control technical systems that make use of the latest advances in radio electronics [1, 2]. Automation of radar information processing is one of the priority directions of development in the field of radar, which became possible due to increase of performance of specialised information processing systems and development of statistical theory of measurements and decision-making.

Two-coordinate and three-coordinate surveillance radars ensure successful solution of tasks of detection, guidance, target designation, airspace reconnaissance, air traffic control and air traffic management (ATC). Lookout radars are distinguished between primary and secondary (trajectory) stages of radar information processing [3]. In the primary processing tasks of detection, resolution, recognition and measurement of coordinates and motion parameters in one contact with an object within one interval of data update [1]. Trajectory processing improves the quality of radar information and includes the following stages [3, 4, 5, 7]: identification of primary measurements (plots) with trajectories already being tracked; detection and creation of new trajectories; filtering and extrapolation of coordinates and motion parameters of observed objects; removal (resetting) of trajectories from automatic tracking. In surveillance radars, the implementation of trajectory

2000 *Mathematics Subject Classification.* Primary 65C05; Secondary 8180.

Key words and phrases. Monte Carlo method, trajectory, numerical integration method, radar, generalized Gaussian distribution.

* Research was carried out with the support of a grant from the Belarusian Republican Foundation for Basic Research (Project No. T22UZB-009) and the Ministry of Innovative Development of the Republic of Uzbekistan (Project No. IL-4821091588).

processing is significantly complicated by the presence of target-like interfering reflection compensation residuals, called discrete clutters [6, 8, 9]. The appearance of a large number of discrete clutters in the radar view area can lead to false trajectories, the parameters of which are sometimes comparable to real aerodynamic aircraft. Figure 1 shows an example of a real-world S-band ATC surveillance radar. There is a lot of interference, which creates false trajectories that interfere with the observation of trajectories of real airborne objects.

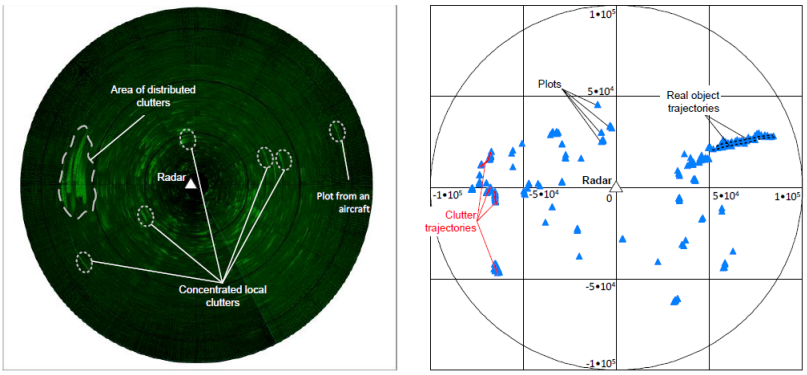

FIGURE 1. Radar indicator (a), plots and trajectory results accumulated over 30 operational scans (b) of the real 2D S-band ATC surveillance radar.

In surveillance radars, clutter maps are used to counteract discrete clutter (see, for instance [2, 6, 10, 11, 12, 13]). However, these methods are not always ineffective, as the main feature to distinguish aerial vehicles from discrete clutters is their trajectory features.

To distinguish the trajectory of a real airborne object from the trajectory of a discrete clutter, it is necessary to calculate the likelihood ratios of the trajectory features. This requires finding the integral of the product of the a priori and posterior probability density of the trajectory parameter vector, conditional on the target class and the input influence model. The choice of a priori probability density of the vector of trajectory parameters must take into account the altitude-velocity characteristics of targets and sources of discrete clutters. The solution of such a problem by analytical integration methods is significantly complicated. An important problem in this case is the closest possible mathematical description of altitude-velocity characteristics of real objects and on their basis representation of a priori probability density function.

This paper introduces the notion of a physically realisable trajectory and substantiates the use of generalised normal distributions [15] that allow us to keep the a priori probability densities of trajectory parameters uniform in the region of their admissible values with a simultaneous smooth decline at their boundaries.

A posteriori probability density of the vector of trajectory parameters determined by a non-linear transformation over the posterior probability density of the

state vector, estimates of which are calculated in the filtering and extrapolation unit [16, 18]. The complexity of calculating the posterior probability density of trajectory parameters and finding integral of the product of this density with a priori probability density determines the transition to numerical integration and approximation methods. The requirements for such methods are the following: high approximation accuracy (finding a numerical solution), high speed of convergence to the true value and simplicity of practical implementation. Numerical methods based on discrete grid and Monte Carlo approximation methods meet these requirements [17, 18, 19]. These methods have a high efficiency when applied to various applications of nonlinear discrete filtering, which is proved by a large number of foreign and domestic publications. In this paper, the choice of the Monte Carlo method is justified, which is associated with a smaller amount of calculations and speed of convergence to the true value, in comparison with the methods based on a discrete grid [18].

2. Features of the Automatic Track Deleting Phase

In most trajectory processing algorithms that have been implemented, the main indication for deciding to drop a trajectory from automatic tracking is the appearance of some sequence of missing (missing) marks associated with this trajectory in its gates while tracking. To account for such a sequence, a criterion is used that says that a trajectory must be missed if a threshold series of n consecutive missing plots appears [3]. The main problem in this case is the value of the parameter n, which in practice is chosen in the range from 3 to 5 (see, for instance [3, 4]). However, this approach does not allow to discard false trajectories, which occur when a large number of interfering marks (target-like compensation residuals from volumetrically and surface-distributed interfering reflections) are observed (see, for instance [4, 6]). In this case, improving the quality of secondary processing at the object trajectory reset stage, along with the calculation of skip marks, is possible by considering a priori information (a posteriori estimation density at the previous stage) about possible values of trajectory parameters and evaluating the consistency of filtering algorithms - i.e., by checking the physical feasibility of the trajectory.

3. Indicators of Physically Realisable Trajectories of Observed Aerial Objects

Physically realizable trajectory is such a trajectory of an object, the aggregate of single coordinate estimates of which falls within the range of possible values of trajectory parameters of radar observation objects and corresponds to one of the possible models of input impact, typical for escorted classes of objects. For example, the speed of aerodynamic aircrafts observed by the all-sky radar is in the range of 35 to 850 m/s (see, [1]). In addition, the trajectory processing algorithm must take into account all types of input impact models characteristic of the observed objects.

The distribution of trajectories of objects of different classes by altitudes and velocities (and sometimes by their derivatives) is the most commonly used feature of selection target and discrete clutter. The additional use of models of the

reference and disturbance effects corresponding to the observed objects on coordinate and motion parameter measurements, combined with estimates of trajectory parameters, makes it possible to reduce the average time for making a correct decision about the class of the observed object while maintaining fixed values of false recognition probabilities (see, [8]).

The distribution of discrete clutters by altitude and velocity is determined by the movement pattern of the clutter sources. Figure 2 shows the altitude-velocity characteristics of discrete clutter sources for an eastern European mid-continental climate. Clouds form in the troposphere. The lower boundary of the clouds is 200 m, the upper boundary coincides with the upper boundary of the troposphere and can reach 12 km. Average velocity and predominant direction of cloud movement coincides with average wind speed and its direction; the scatter of velocities and directions of cloud movement is determined by atmospheric turbulence and scatter of directions of air streams by altitudes. For the East-European regions the maximum wind velocity in the surface layer does not exceed 35 m/s (see, [8]). Velocities of "angel echo" sources are close to cloud velocities and their altitudes range from 100 m to 3000 m (see, [8]). Surface distributed reflectors and concentrated objects are stationary. Their height is determined by the altitude of the terrain and the reflector itself relative to the phase centre of the radar antenna.

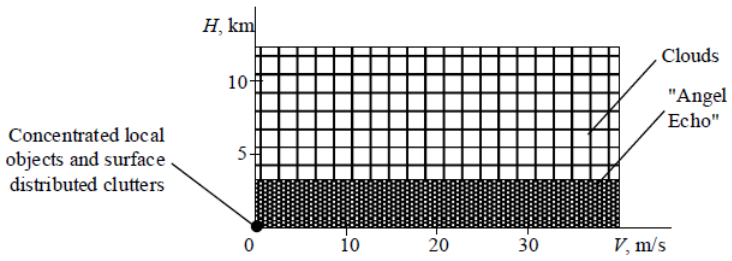

FIGURE 2. Altitude-velocity characteristics of discrete clutter sources for an eastern European mid-continental climate

In order to simplify the decision-making procedure, the allowed range of heights and speeds for real objects to be analysed is limited to four lines: minimum height, maximum height, minimum speed and maximum speed.

An example of the altitude-velocity characteristics of real aircraft (excluding low-speed aircraft such as: helicopter, balloon, hang glider and small unmanned aerial vehicle) is shown in Figure 3. These characteristics in turn depend on the aerodynamic and thrust characteristics of the aircraft. Thus, the maximum altitude is determined by the permissible pressure in the air intake channels, and the lower one by the structural strength limit. The minimum permissible flight speed is determined by the lowest sustained flight speed at a given altitude, preventing the aerodynamic aircraft from stalling, and the maximum permissible flight speed is the highest sustained flight speed at a given altitude, at maximum engine operation mode, ensuring the flight safety of the aircraft.

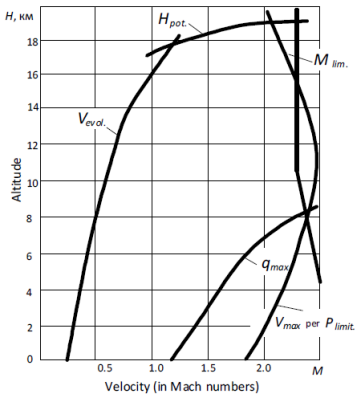

FIGURE 3. Altitude-velocity characteristics of real aerodynamic objects (where H_{pot}−potential attainable altitude; M_{lim}−Mach number airspeed limit; V_{evol}−the minimum speed at which an aircraft can evolve, q_{max}−maximum speed pressure; V_{max} per P_{limit}−maximum speed at maximum thrust).

Thus, there are trajectory differences between aerodynamic objects and discrete jammers in terms of their altitude-velocity characteristics. Aerodynamic objects can fly at altitudes from 0.05 to 25 km, while discrete jammers can fly from 0 to 12 km. The range of flight speeds for aerodynamic objects is between 50...70 (on landing) and 850 (or more) m/s, and for discrete jammers from 0 to 35 m/s. Thus, an aerodynamic object can only be distinguished from discrete jammers by its altitude if it flies at altitudes above 12 km. The velocity ranges of aerodynamic objects and discrete jammers do not overlap (discrete jammers up to 35 m/s and aerodynamic objects from 50 m/s), which makes it possible to distinguish aerodynamic objects against discrete jammers and use this information for evaluation of physical realizability of real air object trajectory (see fig.4).

4. Features of using a generalised normal distribution in describing a priori features of the physical feasibility of a trajectory

To calculate the likelihood ratios for the physical feasibility of a trajectory, it is necessary to find the integral of the product of the a priori and posterior probability density of the trajectory parameter vector, conditional on the object class (two object classes - aerodynamic object and discrete clutter) and the object motion model. The choice of the a priori probability density of the trajectory parameter vector must take into account the altitude-velocity characteristics of aerodynamic objects and discrete clutter sources described in the article above.

If one-dimensional case is considered (e.g., only in height of aerodynamic object and discrete interference source), then most often uniform distribution law is used to describe the a priori features (see Figure 5, *a*)). The input data for the presented example are as follows: the range of possible velocities for the "aerodynamic object" class is 35 to 850 (or more) m/s, for the "discrete clutter" class it

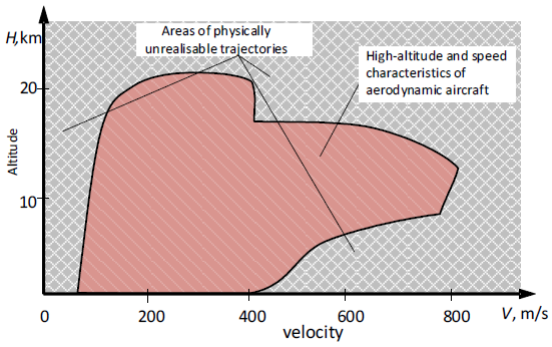

FIGURE 4. Conditions for physical feasibility of a real aircraft trajectory based on its altitude-velocity characteristics.

is 0 to 35 m/s; the uniform distribution law parameters for the "discrete clutter" is a = 0, b = 35; for the "aerodynamic object", a = 35, b = 850. Despite the simplicity of representation, uniform distribution densities are characterized by a sharp limitation of the boundaries of the trajectory parameter value ranges, which leads to jumps in the likelihood ratios, transients in these values and increases the decision time on the physical feasibility (not feasibility) of the trajectory.

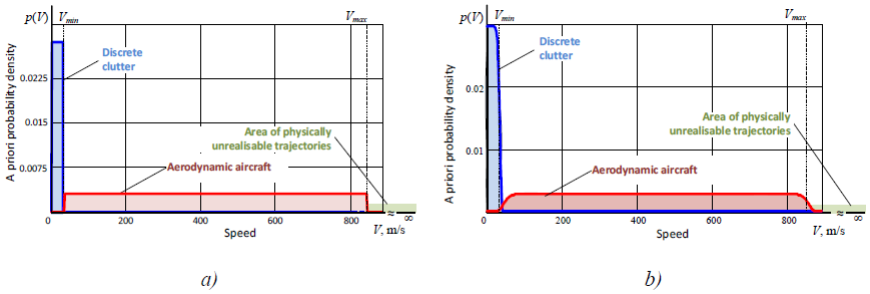

FIGURE 5. Examples of representations of a priori probability densities of trajectory attributes of physical realisability of a trajectory: a) using a uniform distribution law; b) using a generalised normal probability density.

In order to eliminate the negative impact of the jump change in the likelihood ratio of the trajectory features on the decision-making procedure and to ensure uniformity of a priori probability densities of the trajectory parameters in the region of admissible values, their description is possible by means of left-to-zero truncated generalized normal distributions. The generalized normal distribution, examples of which are shown in Figure 6, is a parametric family of symmetric distributions (see, [15]).

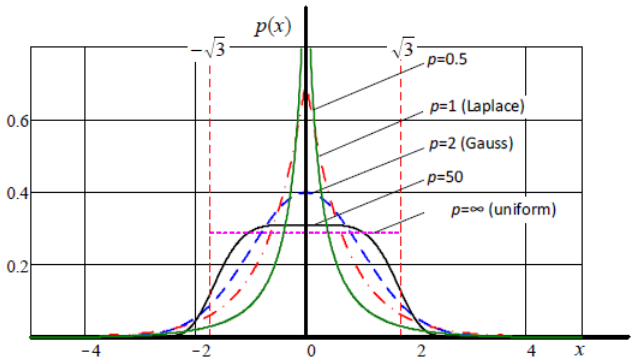

FIGURE 6. Centred generalised Gaussian probability density function with unit variance for different values of the shape parameter.

Fig.6 Centred generalised Gaussian probability density function with unit variance for different values of the shape parameter.

The probability density $p_{GGD}(x)$ of random variables obeying this family is given by the formula (see, [15]):

$$p_{GGD}(x) = \frac{1}{2\Gamma\left(1+1/p\right)A\left(p,\sigma\right)} e^{-\left(\left|\frac{x-\mu}{A(p,\sigma)}\right|\right)^p},$$

where $\Gamma(x) = \int_0^\infty t^{x-1}e^{-t}dt$ - Gamma function;

$A\left(p,\sigma\right) = \sqrt{\left(\sigma^2\Gamma\left(1/p\right)\right)/\Gamma\left(3/p\right)}$ - distribution parameter;

$\sigma-$ standard deviation;

$\mu-$ mean;

$p-$ form parameter.

The generalised normal distribution has three special cases, illustrated in Figure 5:

$p=1-$ the distribution is transformed into a Laplace distribution;

$p=2-$ the distribution is transformed into a Gaussian (normal) distribution;

$p=\infty-$ the distribution converges to a uniform distribution law on the interval $(\mu-\sqrt{3}\sigma, \mu+\sqrt{3}\sigma)$ (see, [15]).

Since the altitutude-velocity characteristics cannot be in the region of negative values, it therefore requires the use of a priori densities truncated to the left at zero. The probability density of a generalised Gaussian distribution truncated to the left at zero will be:

$$p_{TGGD}(x) = p_{GGD}(x) \Bigg/ \left(1 - \int_{-\infty}^{0} p_{GGD}(x)dx\right).$$

Figure 5, *b*), shows an example of generalised normal distributions, truncated to the left at zero, used to describe the a priori densities of the total velocity distribution (raw data: the range of possible velocities of the aerodynamic object and discrete clutter correspond to the figure ; the density parameters for discrete interference are $\sigma = 20$, $\mu = 0$, $p = 8$ for "aerodynamic object" –$\sigma = 235$, $\mu = 45$, $p = 40$ As can be seen from Figure 5, *b*) the use of generalised normal distributions maintains uniform a priori probability densities of trajectory parameters in the range of their admissible values, with a simultaneous smooth decline at their boundaries.

5. Features of Using the Monte Carlo Method for Probability Density Approximations in Radiolocation

Although it is possible to represent analytically the components of the integral from the a priori and posterior probability densities of the trajectory features, it is difficult to express its first form through analytical functions. This problem can be eliminated by using numerical integration methods. The choice of the Monte Carlo integration method is due to the advantages of this method over the others (see, [18, 19]): direct accounting of the influence of nonlinear transformations on the approximated density, simple implementation and high convergence rate.

The Monte Carlo method is a universal method for the approximate calculation of integrals I of high multiplicity from some non-random multidimensional function $g(\alpha)$ (see, [18]):

$$\int\limits_{\mathbb{R}^{n_\alpha}} g(\alpha)d\alpha = \int\limits_{\mathbb{R}^{n_\alpha}} \frac{g(\alpha)}{q(\alpha)} q(\alpha)d\alpha. \tag{5.1}$$

To calculate the integral it is necessary (see, [18]):

1) obtain N independent random counts α^i (so-called Monte Carlo random samples (particles)), where i is the number of random argument generated by the random number sensor ($i = \overline{1,N}$; $N >> 1$) distributed in the region $\mathbb{R}^{n_\alpha}$ with some distribution density $q(\alpha)$ (where $n_\alpha-$dimension of vector α);

2) determine at points α^i values of function $g(\alpha^i)$ and probability density $q(\alpha^i)$;

3) find numerical value of integral by formula:

$$I_N = \frac{1}{N}\sum_{i=1}^{N} \frac{g(\alpha^i)}{q(\alpha^i)}. \tag{5.2}$$

For independent samples α^i, the estimate I_N is unbiased and, according to the law of large numbers, converges in probability to the true value (5.1). The variance of the estimation error of the integral (5.2) in this case is defined by the expression:

$$D_N = \frac{1}{N}\sum_{i=1}^{N} \left(\frac{g(\alpha^i)}{q(\alpha^i)} - I_N \right)^2. \tag{5.3}$$

From (5.3) it can be seen that that the order of convergence error estimate of the Monte Carlo method is proportional to relation $1\Big/\sqrt{N}$. Expression (5.2) contains as a free parameter, the probability density function $q(\alpha)$ of random samples α^i. Its choice is dictated by the requirement of minimizing the variance (5.3) by reducing the dispersion of the ratio $g(\alpha)/q(\alpha)$ the probability density $q(\alpha)$

value is considered to be admissible with respect to the function $g(\alpha)$, if condition (see, [18]) is fulfilled:

$$q(\alpha) > 0 \quad \text{for all} \quad \alpha \in \mathbb{R}^{n_\alpha}, \quad \text{in which} \quad |q(\alpha)| > 0. \tag{5.4}$$

The scatterplot of the random values of the density $q(\alpha)$ must overlap the area of all possible values of the integrating function $g(\alpha)$. The variance of the integration error will be minimal if the condition is satisfied:

$$q(\alpha) \propto |g(\alpha)|\,. \tag{5.5}$$

Dispersion minimisation (5.3) is explained as follows: when conditions (5.4) and (5.5) are satisfied, regions with a large value of the function $|g(\alpha)|$ will be the most likely to generate random samples. These samples will contribute more significantly to the I_N estimate than the others, for which $|g(\alpha)|$ is negligible.

The set of random samples distributed according to density $q(\alpha)$ for which conditions (5.4) and (5.5) are satisfied is called Importance Sampling and the probability density is called Importance Density (see, [19]).

6. Monte Carlo Approximation of an Arbitrary Probability Density Function

Let a non-random function $g(\alpha)$ be represented as the product of some pre-specified function $f(\alpha)$ and a probability density $p(\alpha)$ positively defined on a domain $\mathbb{R}^{n_\alpha}$ (see, [19]):

$$g(\alpha) = f(\alpha)p(\alpha). \tag{6.1}$$

If the upper boundedness condition of the ratio $g(\alpha)/q(\alpha)$ is satisfied, expression (5.1) will be written as [19]:

$$I_N = \frac{1}{N}\sum_{i=1}^{N} f(\alpha^i)\frac{p(\alpha^i)}{q(\alpha^i)} = \frac{1}{N}\sum_{i=1}^{N} f(\alpha^i)\tilde{w}^i, \tag{6.2}$$

Where $\tilde{w}^i = \dfrac{p(\alpha^i)}{q(\alpha^i)}$– irregular weights.

The use of non-normalised weights $\tilde{w}^i$ is converted to normalised weights [18]:

$$w^i = \frac{\tilde{w}^i}{\sum\limits_{j=1}^{N}\tilde{w}^j}, \quad \sum_{i=1}^{N} w^i = 1. \tag{6.3}$$

Expression (6.1) with reference to (6.3) will be written as:

$$I_N = \sum_{i=1}^{N} f(\alpha^i)\frac{\tilde{w}^i}{\sum\limits_{j=1}^{N}\tilde{w}^j} = \sum_{i=1}^{N} f(\alpha^i)\tilde{w}^i. \tag{6.4}$$

When using the delta function $\delta(\alpha)$ instead of $f(\alpha)$, the probability density function $p(\alpha)$ can be approximated by a weighted sum (due to the filtering property of the delta function) (see, [19]):

$$p(\alpha) = \frac{1}{N}\sum_{i=1}^{N} \tilde{w}^i \delta(\alpha - \alpha^i) = \sum_{i=1}^{N} w^i \delta(\alpha - \alpha^i). \tag{6.5}$$

The minimum variance of the approximation error $p(\alpha)$ will be observed when the equality $q(\alpha) = p(\alpha)$ is satisfied. In nonlinear Bayesian filtering the pairs $\{\alpha^i, w^i\}_{i=1}^N$ are called particles. Here α^i is the coordinate of the i-th particle and w^i is its weight. In the simplest case the weight is chosen equal to the value of density $\delta(\alpha)$.

Example of Monte Carlo approximation of one-dimensional probability density function. Let the density for a one-dimensional random variable x be defined as Gaussian (expectation equal to zero and variance equal to $D = 169$). We know that the probability density for the square of a Gaussian random variable with RMS D is:

$$f_y(y) = \frac{1}{\sqrt{2\pi y D}} e^{\left(-\frac{y}{2D}\right)}, \quad y > 0. \tag{6.6}$$

This needs to be proved using the Monte Carlo approximation method (see Figure 7). The proof was carried out in three stages. In the first stage, random Monte Carlo samples were generated (the number of random samples was 3074, in order to provide a relative error value of 5% and a confidence level of 0.95) within the allowable values of the random variable x, with weights equal to the probability density function, as shown in the upper left part of Figure 7). At the second stage, weights were normalised and the initial distribution law was checked for consistency with the Monte Carlo distribution obtained by solving the problem of statistical series alignment followed by the Pearson's χ^2 test, as shown in the middle section of Figure 7. As a result of the calculations, it was determined that, with 7 degrees of freedom, the confidence interval was $p = 0.95$. The third step was a non-linear Monte Carlo transformation $y = x^2$ over random samples, followed by a Monte Carlo test for consistency with the distribution law (6.6). The calculation showed that, with 7 degrees of freedom, the confidence was also $p = 0.95$ for condition (6.6). Thus, the statement was true.

An example of approximation of two-dimensional probability density function by Monte Carlo method. As an example, we considered the classical radiolocation's problem of finding the joint probability density function for the amplitude and phase of an oscillation generated by the rotational motion of a point with coordinates x_1, x_2 around the origin. For different values of parameters of random variables x_1, x_2 there will be different kinds of distribution of amplitude and phase. As an example, we considered the simplest case of centred independent random variables with the same unit variance. In this case, the amplitude A will have a Rayleigh distribution density and the phase will be uniformly distributed. The Monte Carlo approximation procedure for the two-dimensional probability density function is similar to the one-dimensional probability density function and is

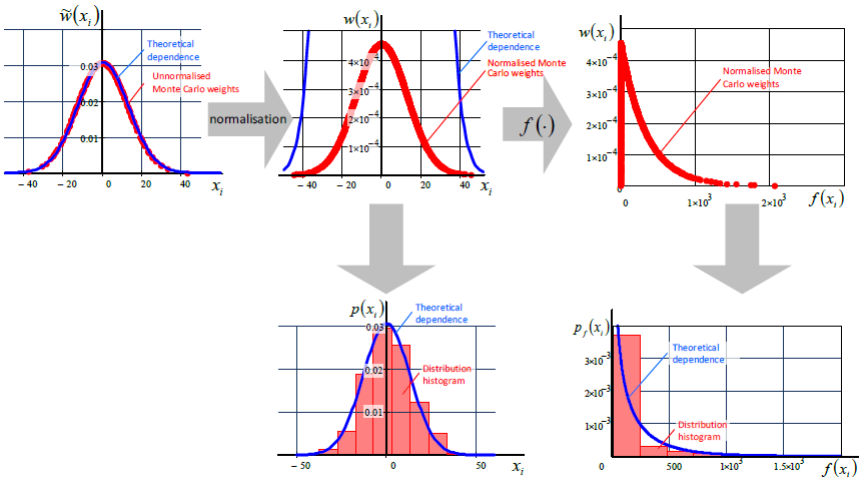

FIGURE 7. Example of Monte Carlo approximation of a probability density function (univariate case).

shown in Figure 8. As can be seen from the figure, after a non-linear transformation over the generated Monte Carlo random samples, the law is checked against the obtained Monte Carlo method.

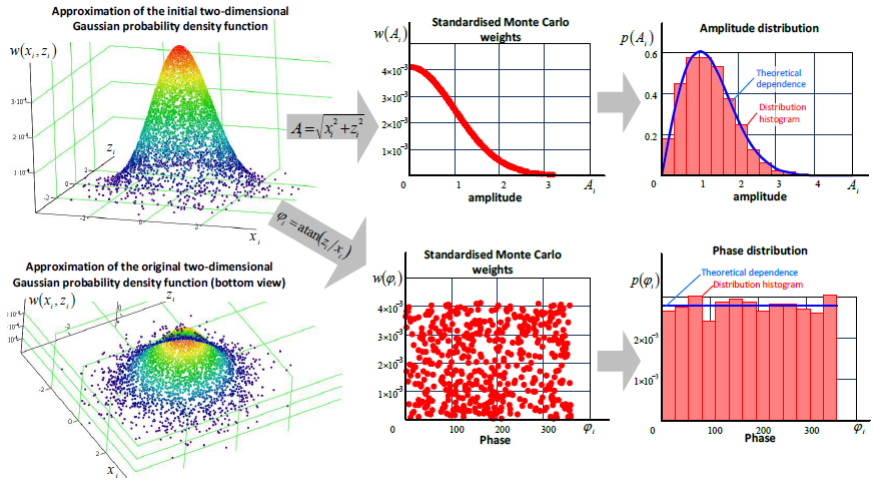

FIGURE 8. Example of Monte Carlo approximation of a probability density function (two-dimensional case).

Thus the numerical Monte Carlo method has a high approximation accuracy (finding a numerical solution) and is easy to implement in practice. Compared

to grid-based methods, the Monte Carlo method is less computationally intensive and has a higher rate of convergence to the true value.

7. Method for Verifying a Physically Realisable Trajectory

Based on the approaches proposed above, the device for checking physical feasibility and selecting trajectory signs was implemented, which consists of the following elements (see Fig. 9): block of approximation of a posteriori probability densities; block of evaluation of trajectory consistency and probability of physical feasibility, decision-making device on assigning a sign "physically unrealizable trajectory".

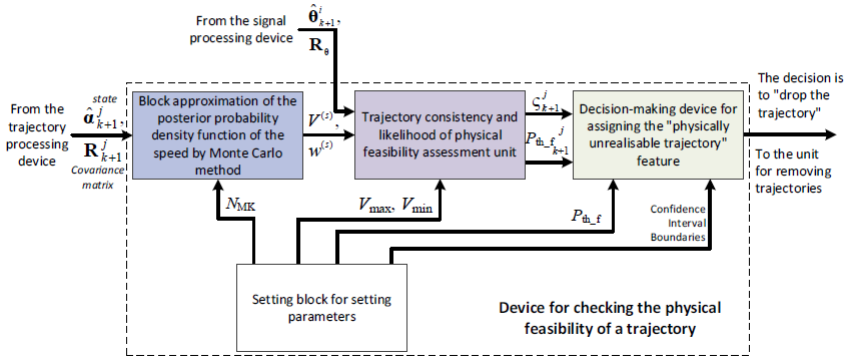

FIGURE 9. Device for checking the physical feasibility of a trajectory.

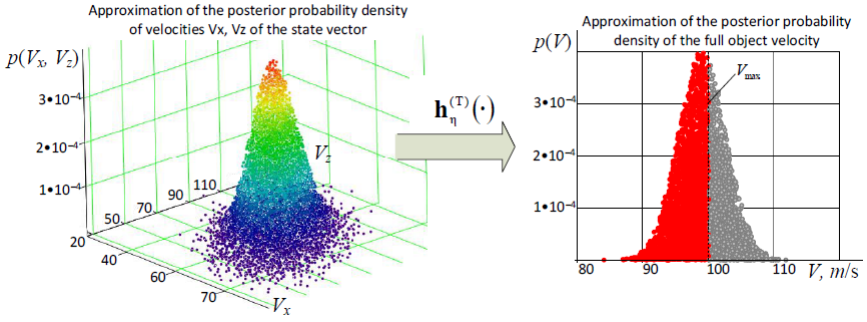

FIGURE 10. Example of Monte Carlo approximation of the full velocity probability density.

The proposed methodology for checking the physical feasibility of a trajectory at the stage of trajectory reset from automatic tracking is reduced to the calculation

of the likelihood ratio $V_f(V_{k+1}^{(j)})$ based on the trajectory parameters at the current $(k+1)$-survey of the radar:

$$L_{Tp}(V_{k+1}^{(j)}) = \int_{V_{\min}}^{V_{\max}} p(V_{k+1}^{(j)}) p(V_{k+1}^{(j)} \Big| \mathbf{\Theta}_{k+1}^{(j)}) dV_{k+1}$$

where $V_{k+1}^{(j)} = \mathbf{h}_V^{(T)}(V_{k+1}^{(j)})-$is the full velocity of the object for the $j-$th trajectory on the $k+1-$survey, related to the state vector $\alpha_{k+1}^{(j)}$ via the functional transformation $\mathbf{h}_\eta^{(T)}(\cdot)$ (for the two-dimensional case see Figure 10 for an example);

$p(V_{k+1}^{(j)})-$is the a priori probability density of total velocity $V_{k+1}^{(j)}$ for the $j-$th trajectory on the $k+1-$ survey at the set (first to $k+1-$th) $\mathbf{\Theta}_{k+1}^{(j)}$ of radar plots of the detected object;

$p(V_{k+1}^{(j)} \Big| \mathbf{\Theta}_{k+1}^{(j)})-$is the posterior total velocity density $V_{k+1}^{(j)}$ for the $j-$th trajectory on the $k+1-$survey at the set (first to $k+1-$th) $\mathbf{\Theta}_{k+1}^{(j)}$ of radar marks of the detected object;

$V_{\max}^{\min}$ minimum and maximum full velocity.

The developed methodology for verifying the physical feasibility of a trajectory at the stage of trajectory reset from automatic tracking includes the following sequence of actions (on the example of the $j-$th trajectory, the upper index j is omitted):

1. Monte Carlo approximation of the posterior probability density function of the state vector $p(\alpha_{k+1} | \mathbf{\Theta}_{k+1})$ on the $k+1-$survey by a set of N_{MC} random Monte Carlo particles $\alpha_{k+1}^{(s)}$.

2. Approximation of the posterior probability density function of the full velocity distribution $p(V_{k+1}^{(j)} \Big| \mathbf{\Theta}_{k+1}^{(j)})$ by a non-linear transformation $\mathbf{h}_V^{(T)}(\alpha_{k+1}^{(s)})$ over the approximated density function .

3. determine the value of the likelihood ratio by calculating the numerical value of integral $L_F\left(V_{k+1}^{(j)}\right)$ using the Monte Carlo method.

4. Assess the physical feasibility of the trajectory by comparing $L_F(V_{k+1}^{(j)})$to a pre-set threshold value L_{th}.

5. Calculate the consistency of the estimation of the filtering and extrapolation device according to (see, [7]) and check that it falls within a given confidence interval.

6. The evaluation of the final physical feasibility of the trajectory (for the case of "physically unrealizable trajectory") is performed according to the calculated value of the likelihood ratio (5.1), taking into account the value of the filtering device consistency.

8. Conclusion

The paper considers the problem of false trajectories, which significantly complicate the process of radar observation of useful real airborne objects. It was shown that false trajectories can be formed both randomly (by noise) and from

discrete interference. To combat false trajectories, it is necessary to carry out the consistency check on the set of trajectory marks and take into account the trajectory differences of interference from useful objects. In order to take into account trajectory differences one must form an integral of the product of a priori features and posterior probability density. In this paper we propose a method of Monte Carlo approximation of posterior probability density function and description of a priori distributions of trajectory features of selection by generalized Gaussian density function truncated to zero to eliminate step change of probability ratio for trajectory features. The advantage of calculating integrals included in the likelihood ratios using the trajectory features by the numerical Monte Carlo integration method is substantiated, which will allow taking into account the a priori density form of any complexity, and the required accuracy of such likelihood ratio calculations will be determined by the number of random Monte Carlo samples.

Acknowledgment. Research was carried out with the support of a grant from the Belarusian Republican Foundation for Basic Research (Project No. T22UZB-009) and the Ministry of Innovative Development of the Republic of Uzbekistan (Project No. IL-4821091588)).

References

1. Skolnik, M.: *Radar Handbook*, Third Edition 3rd ed., McGraw-Hill, 2008.
2. Richards M. A., Scheer J. A., Holm W. A.: *Principles of Modern Radar: Basic Principles*, Edison, NJ: Scitech Publ., USA, 2010.
3. Blackman S., Popoli R.: *Design and Analysis of Modern Tracking Systems*, London: Artech House, Boston, 1999.
4. Solonar, A. S., Khmarski, P. A.: Main Problems of Trajectory Processing and Approaches to Their Solution Within the Framework of Multitarget Tracking, in: *J. Phys.: Conf. Ser.* **1864**, part 1 (2021) 1–7.
5. Solonar, A. S., Khmarski, P. A.: General Construction Principles and Performance Features of Trajectory Processing by Data From One Radar Data Source, in: *J. Phys.: Conf. Ser.* **1864**, part 1 (2021) 1–8.
6. Solonar, A. S., Khmarski, P. A.: Quality Indicators of Devices for Tajectory Processing of Radar Information and Methods of Their Testing, in: *J. Phys.: Conf. Ser.* **1864**, part 1 (2021) 1–7.
7. Bar-Shalom Y., Li X. R., Kirubarajan T: *Estimation with Applications to Tracking and Navigation*, New York: A Wiley-Interscience Publication, New York, 2001.
8. Barton D. K.: *Radar Equations for Modern Radar*, London: Artech House, Boston, 2013.
9. Artemiev V. M., Kostromitsky S. M., Naumov A. O.: Detection of signals of moving objects based on the time selection method, *Proceedings of the National Academy of Sciences of Belarus. Physical-Technical Series* **66**, No. 3 (2021) 335–342.
10. Melvin W. L., Scheer J. A.: *Principles of Modern Radar: Advanced Techniques*, Edison, NJ: Scitech Publ., 2013.
11. Musicki D., Evans R.: Clutter map information for data association and track initialization, *IEEE Transactions on Aerospace and Electronic Systems* **40**, No. 2 (2004) 387–398.
12. Li X. R., Bar-Shalom Y.: Design of an interacting multiple model algorithm for air traffic control tracking, *IEEE Transactions on Control Systems Technology* **1**, No. 3 (1993) 186–194.
13. Kirubarajan T., Bar-Shalom Y.: Probabilistic data association techniques for target tracking in clutter, *Proceedings of the IEEE* **92**, No. 3 (2004) 536–557.
14. Song, T. L., Kim Y. W., and Musicki, D.: Distributed (nonlinear) target tracking in clutter, *IEEE Transactions on Aerospace and Electronic Systems* **51**, No. 1 (2015) 654–668.

15. Nadarajah, S.: A generalized normal distribution, *Journal of Applied Statistic* **32**, No. 7 (2005) 685–694.
16. Li, X.R.: Survey of maneuvering target tracking. Part III: Measurement models, in: *Proceedings of SPIE Conference on signal and Data processing of small target* **4473**, (2001) 1–24.
17. Johnson A. A., Ott M. Q., Mine D.: *Bayes Rules!: An Introduction to Applied Bayesian Modeling 1st Edition*, Chapman & Hall/CRC Texts in Statistical Science, 2021.
18. Bergman, N.: *Recursive Bayesian estimation. Navigation and Tracking Applications*, Linkoping: Linkoping University, Sweden, 1999.
19. Ristic, B.: *Beyond the Kalman Filter. Particle Filters for Tracking Applications*, London: Artech House. Boston, 2004.

Andrei Sergeevich Solonar: Department of Automation, Radar and Transceiver Devices, Military Academy of the Republic of Belarus, Minsk, Belarus
Email address: andssnew@yandex.ru

Petr Alexandrovich Khmarski: Laboratory of Radiotomography, Institute of Applied Physics, National Academy of Sciences of Belarus, Minsk, 220072, Belarus
Email address: pierre2009@mail.ru

Alexander Olegovich Naumov: Laboratory of Radiotomography, Institute of Applied Physics, National Academy of Sciences of Belarus, Minsk, 220072, Belarus
Email address: naumov@iaph.bas-net.by

Davron Aslonqulovich Juraev: 1. Department of Scientific Research, Innovation and Training of Scientific and Pedagogical Staff, University of Economics and Pedagogy, Karshi, 180100, Uzbekistan; 2. Department of Mathematics, Anand International College of Engineering, Jaipur, 303012, India
Email address: juraevdavron@yandex.com

Bobomurod Muxammadkarimovich Muxammedov: Department of Radioelectronic Equipment, Higher Military Aviation School of the Republic of Uzbekistan, Karshi, 180117, Uzbekistan
Email address: airforce@umail.uz